Journal of Inflammation Research

Dovepress
Taylor & Francis Group

Open Access Full Text Article

ORIGINAL RESEARCH

Unfractionated Heparin Attenuates Histone-Induced Pulmonary Endothelial Glycocalyx Injury: A Preliminary Study on the Roles of the ROCK Pathway and Heparanase-1

Xinghua Li, Yawen Chi, Mengke Zhuo, Xin Li, Chengrui Zhu, Xu Li

Department of Critical Care Medicine, The First Affiliated Hospital, China Medical University, Shenyang, Liaoning Province, People's Republic of China

Correspondence: Xu Li, Department of Critical Care Medicine, The First Affiliated Hospital, China Medical University, North Nanjing Street 155, Shenyang, Liaoning Province, 110001, People's Republic of China, Tel +86 024 83282261, Fax +86 024 83282631, Email vincentzh002@outlook.com

Purpose: This study aims to investigate the role of the Rho-associated kinase (ROCK)-1 pathway, with the involvement of heparanase (HPA)-1, in histone-induced disruption of the endothelial glycocalyx and the protective effects of unfractionated heparin (UFH).

Methods: Human pulmonary microvascular endothelial cells (HPMECs) were cultured in vitro and divided into 4 groups: control group, histone group, histone+UFH group, and histone+ROCK inhibitor (Y27632) group. The control group was treated with phosphate buffer solution (PBS). Histone group was treated with histone 50μg/mL for 1 hour. UFH 10 IU/mL and Y27632 10 uM were added 30 min before exposure to histones.

Results: UFH attenuated histone-induced permeability changes of HPMECs. UFH reduced histone-induced syndecan-1 shedding and the depolymerization of Ace-tubulin and β-tubulin. UFH inhibited histone-induced decrease in syndecan-1 and Ace-tubulin. UFH inhibited histone-induced expression, re-distribution and secretion of HPA-1. UFH reduced histone-induced expression of ROCK-1 and phosphorylated myosin light-chain (p-MLC) in HPMECs.

Conclusion: UFH protects the glycocalyx and endothelial barrier while inhibiting histone induced HPA expression, perinuclear distribution, and secretion, with the involvement of the ROCK pathway.

Keywords: histone, unfractionated heparin, glycocalyx, heparanase, Rho-associated kinase

Introduction

Sepsis is life-threatening organ dysfunction due to a dysregulated host response to infection and is an important global health problem.[1] There are approximately 50 million cases of sepsis per year, resulting in 11 million deaths worldwide and accounting for 20% of total mortality.[2] The pathophysiology of sepsis involves the systemic inflammatory cascade and coagulation activation, which leads to tissue hypoxia, multiple organ dysfunction syndrome (MODS), and even death. Therefore, it is essential to explore the underlying pathophysiological pathways and possible therapeutic strategies for sepsis.

Under normal conditions, histones bind stably with DNA.[3] However, under pathological conditions, histones are released from tissue cells through NETosis, apoptosis, and necrosis, which mediate inflammatory reactions, coagulation activation, and organ damage.[4–6] Moreover, extracellular histones serve as biomarkers for the progression of sepsis and other inflammatory diseases.[7] Our previous research demonstrated that histones mediate glycocalyx disruption, coagulation activation, and acute lung injury in mice.[6,8]

The vascular endothelial glycocalyx layer (EGL) is the first barrier separating blood from tissues and organs and plays an important role in maintaining cell permeability, inflammatory response, and coagulation function.[9,10] The EGL is mainly composed of proteoglycans (PG), glycoproteins and glycosaminoglycans (GAG). Syndecan is a type of proteoglycan, which consists of four syndecan subtypes. Syndecan-2 and -3 exert complex antagonistic effects (both anti- and

https://doi.org/10.2147/JIR.S573499
Received: 18 October 2025
Accepted: 25 May 2026
Published: 8 June 2026

pro-inflammation), though their mechanisms remain unclear. Syndecan-4 is upregulated by inflammatory mediators and exerts beneficial pro-inflammatory effects.[11–13] Syndecan-1 expression is downregulated by various inflammatory mediators Interleukin (IL)-1β, IL-6, Lipopolysaccharide (LPS), histones,[14,15] although upregulation by Transforming Growth Factor-β1 (TGF-β1) and Tumor Necrosis Factor-α (TNF-α) has also been reported.[16] Importantly, shed syndecan-1 fragments have dual effects: they can reduce inflammation (possibly via electrostatic neutralization or indirect signaling) or promote inflammation through Toll-like Receptor 4/ Nuclear Factor-κB (TLR4/NF-κB) activation.[17–19] Thus, glycocalyx shedding serves both as a marker of endothelial injury and as a regulatory mechanism, underscoring the complexity of glycocalyx homeostasis in sepsis. Circulating syndecan-1 levels predict endothelial injury,[20] and septic patients display elevated circulating syndecan-1 levels.[21]

Heparanase (HPA) can specifically degrade endothelial heparan sulfate (HS) chains attached to the glycocalyx.[22] Increased expression of HPA in sepsis results in HS degradation and disruption of the glycocalyx, leading to capillary leakage.[23] Furthermore, it has been demonstrated that cellular kinetic regulation plays an important role in inducing HPA secretion under high glucose conditions.[24] Similarly, LPS can mediate the small GTP-binding protein (RhoA)/Rho-associated kinase (ROCK) pathway and induce phosphorylation of myosin phosphatase target subunit-1 (MYPT-1), leading to cytoskeleton disruption and increased vascular permeability.[25] Our previous studies have also shown that histones can disrupt the endothelial glycocalyx through the HPA pathway and aggravate endothelial permeability, thereby exacerbating inflammation and edema in mouse lung tissues.[8] However, it remains unclear whether the cytoskeleton is involved in histone-induced HPA secretion and glycocalyx destruction.

Heparin, as a commonly used anticoagulant in the clinic,[26] has gradually become the focus of research regarding its non-anticoagulant protective effects.[27,28] In recent years, low-dose unfractionated heparin (UFH) has been found to possess important anti-inflammatory and anti-apoptotic effects.[29,30] For instance, Fu et al[8] demonstrated that UFH attenuated histone-induced glycocalyx injury and protected the vascular endothelium by inhibiting HPA. However, the exact mechanism remains unclear. Therefore, in this study, we aimed to investigate the mechanism by which histones induce glycocalyx damage via the ROCK pathway, with the involvement of HPA, as well as the protective effects of UFH in this process.

Method

Reagents

Human pulmonary microvascular endothelial cell (HPMEC) was obtained from Tongpai Biotechnology Co., Ltd (Shanghai, China). Histone (H9250) was from Sigma-Aldrich (St. Louis, MO, USA). Y-27632 (HY-10071) was from MedChem Express (Monmouth Junction, NJ, USA). UFH (H32022088) was obtained from Changzhou Qianhong Biopharma Co., Ltd. (Changzhou, China). Heparanase1 antibody (polyclonal rabbit anti-human, GTX32650) was from GeneTex (Texas, USA). Acetylated-α-tubulin antibody (monoclonal mouse anti-human, ab24610) was obtained from Abcam (Cambridge, MA, USA). β-tubulin antibody (monoclonal rabbit anti-human, CST 2128), p-MLC (monoclonal rabbit anti-human, CST 3674), and ROCK1 (monoclonal rabbit anti-human, CST 4035) antibodies were purchased from Cell Signaling Technology (CST, Boston, USA). GAPDH antibody (monoclonal rabbit anti-human, 10494-1-AP) was from Proteintech (Hubei, China). CD138/Syndecan-1 (rabbit pAb, A1235) was from Abclonal Biotechnology Co., Ltd. (Hubei, China). Anti-Syndecan-1/CD138 (polyclonal rabbit anti-human, GB115052), HRP-conjugated goat anti-rabbit IgG (H+L, GB23303), HRP-conjugated goat anti-mouse IgG (H+L, GB23301), goat anti-rabbit IgG Alexa488 (GB25303), goat anti-mouse IgG Alexa488 (GB25301), bovine serum albumin (BSA, GC305010) and Prestained Protein Marker II (10–200 kDa, G2058) were obtained from Servicebio Biotechnology Co., Ltd. (Hubei, China). Enzyme-linked immunosorbent assay (ELISA) kit for HPA (ML817310) was purchased from Shanghai Enzyme-linked Biotechnology Co., Ltd. (Shanghai, China). Enhanced BCA Protein Assay Kit (P0010) and FITC-labeled Dextran (MW 40,000, ST2940) were from Shanghai Beyotime Biotechnology Co., Ltd. (Shanghai, China). Dulbecco's modified Eagle's medium (DMEM, high glucose, PM150210) was obtained from Procell Biotechnology Co., Ltd. (Hubei, China). Enhanced chemiluminescence Plus kit (ECL, 180–501) was from Tanon Life Science Co., Ltd. (Shanghai, China).

Cell Culture and Treatments

HPMECs were incubated in Dulbecco's modified Eagle's medium (DMEM) containing 10% fetal bovine serum (FBS) and 1% penicillin/streptomycin solution. The cells were grown at 37°C in a 5% CO_2 atmosphere. The medium was replaced every 1–2 days. After 2 hours of serum-free culture (HPMECs were grown in DMEM without FBS), the cells were treated with histone alone (50 μg/mL) for 1 hour. UFH (10 IU/mL) and Y27632 (10 μM) were added to cells 30 min prior to histone stimulation. The control cells received an equal volume of phosphate-buffered saline (PBS). The doses and time points of histone, UFH and Y27632 were selected based on previous studies and preliminary experiments.[25,31–34]

Measurement of Endothelial Permeability

After adding 100 μL of complete culture medium to the upper chamber and 600 μL to the lower chamber, the transwell inserts (6.5 mm diameter for 24-well plate, 0.4 μm pore size, polycarbonate membrane, without additional matrix coating) were placed in the incubator for 30 minutes to allow stabilization of the culture environment. HPMECs ($1–5 \times 10^5$ cells/well) were then seeded into the upper chamber and cultured under static conditions in the incubator for at least 6 hours to allow initial cell attachment. The medium was changed daily, and cells were cultured for 5 days until reaching 90–100% confluence. The medium was replaced with serum-free medium for 2 h before administration. FITC-dextran (40 kDa) at a concentration of 1 mg/mL was added into the upper chamber for 1 h. Then the medium in the bottom transwell chamber was collected and transferred to a 96-well black plate. The FITC fluorescence intensity was measured using a fluorescence plate reader (Thermo Fisher, USA) at an excitation wavelength of 492 nm and emission wavelength of 520 nm.

Immunofluorescence

HPMECs were cultured on coverslips. HPMECs of passage 5 were utilized upon reaching 60–70% confluence. All cells were fixed with 4% paraformaldehyde or ice-cold methanol. For Ace-tubulin, β-tubulin and HPA, cells were permeabilized with 0.5% Triton X-100. The cells were blocked with 5% bovine serum albumin (BSA) and incubated with primary antibodies at 4°C overnight. Antibody dilution ratios were as follows: rabbit anti-β-tubulin (1:100), rabbit anti-HPA (1:250), rabbit anti-syndecan-1 (1:100), mouse anti-acetylated-α-tubulin (1:400). Then the cells were treated with secondary antibodies respectively: goat anti-rabbit IgG Alexa488 (1:200), goat anti-mouse IgG Alexa488 (1:200). Microscopy was used for image acquisition (ECHO Revolve, California, USA). The fluorescence intensity of Ace-tubulin, β-tubulin, HPA and syndecan-1 was quantitatively analyzed by ImageJ software (National Institutes of Health, Bethesda, MD, USA).

Western Blot

HPMECs of passage 5 were utilized upon reaching 80–90% confluence. The cell protein was extracted using a mixture of RIPA + protease inhibitor cocktail (2:100, Beyotime Biotechnology) + phosphatase inhibitor cocktail (4:100, Beyotime Biotechnology) + EDTA (1:100, Beyotime Biotechnology). The concentration of protein extracts was measured by BCA assay kit. Protein samples were separated by sodium dodecyl sulfate-polyacrylamide gel electrophoresis (SDS-PAGE), electrotransferred to polyvinylidene fluoride (PVDF) membranes, blocked by quick blocking buffer (Beyotime Biotechnology), and treated with primary antibodies at 4°C overnight. Antibody dilution ratios were as follows: rabbit anti-CD138/Syndecan-1 (1:1000), mouse anti-acetylated-α-tubulin (1:1000), rabbit anti-HPA-1 (1:500), rabbit anti-ROCK1 (1:500), rabbit anti-p-MLC (1:1000), rabbit anti-GAPDH (1:10,000). Then the membranes were incubated with HRP-conjugated goat anti-rabbit IgG or HRP-conjugated goat anti-mouse IgG. GAPDH was used as a loading control. The protein bands were visualized with an enhanced chemiluminescence Plus kit (ECL) using a Tanon Gel imaging system. ImageJ software (NIH) was used to quantify the intensity values of the bands. The relative content of target protein was calculated by the ratio of target protein band density to GAPDH band density. Each experiment was repeated three times.

Enzyme-Linked Immunosorbent Assay

HPMECs of passage 5 were utilized upon reaching 80–90% confluence. The cell culture medium was collected and centrifuged at 1000g at 4 °C for 20 min, and the supernatants were collected. Then, the protein secretion levels of HPA in the culture medium of HPMECs were quantified. The process was implemented according to the manufacturer's protocols and repeated three times.

Statistical Analysis

All statistical analyses were performed using GraphPad Prism v8. All values were expressed as mean ± standard deviation (mean ± SD). Multiple group comparisons were performed by one-way analysis of variance (ANOVA) and Tukey's post hoc test. $P < 0.05$ indicated a statistical significance.

Results

UFH Alleviated Histone-Induced Hyperpermeability of HPMECs

The permeability of HPMEC monolayers cultured on Transwell chambers was measured by FITC-dextran penetration across cells. Histone increased endothelial cell permeability (5.41±0.14 μg/mL vs 10.77±0.22 μg/mL, $P < 0.05$), whereas pretreatment with Y27632 (10 μM) for 30 min alleviated the histone-induced hyperpermeability in HPMECs (7.70 ±0.20 μg/mL vs 10.77±0.22 μg/mL, $P < 0.05$). Pretreatment with UFH (10 IU/mL) for 30 min reduced the histone-induced permeability changes in HPMECs (6.49±0.28 μg/mL vs 10.77±0.22 μg/mL, $P < 0.05$) (Figure 1).

UFH Ameliorated Histone-Induced Glycocalyx Shedding and Microtubule Disassembly

Syndecan-1 is the main component of the glycocalyx. Syndecan-1 is degraded from the cell surface into the bloodstream during endothelial injury. As shown in Figure 2A and B, immunofluorescence staining of syndecan-1 showed that the expression of syndecan-1 in endothelial cells decreased significantly in the histone group compared with that in normal cells, whereas Y27632 or UFH restored histone-induced syndecan-1 shedding. Furthermore, we detected syndecan-1

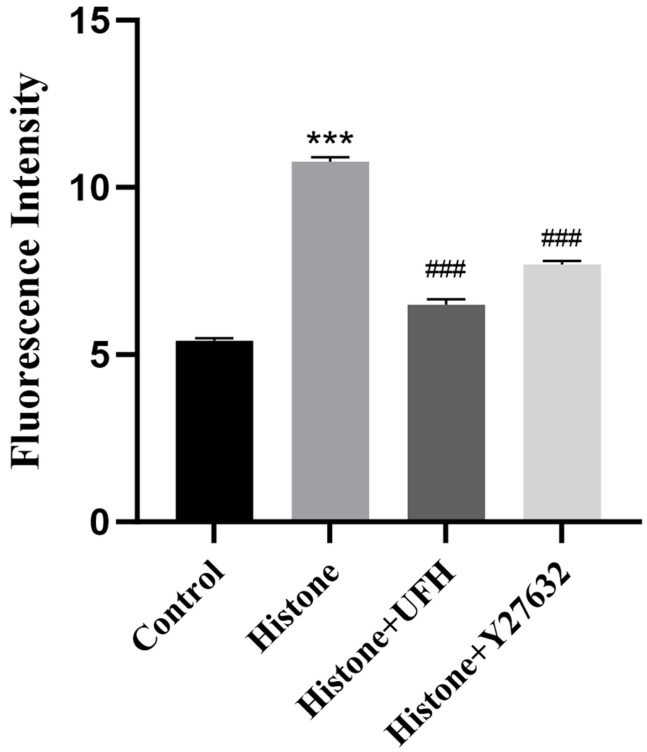

Figure 1 The FITC-dextran penetration method was used to determine the protective effect of UFH or Y27632 on histone-induced increase in permeability of HPMECs. Mean ± SD. n = 3. ***$P < 0.001$, compared with control group; ###$P < 0.001$, compared with histone group.

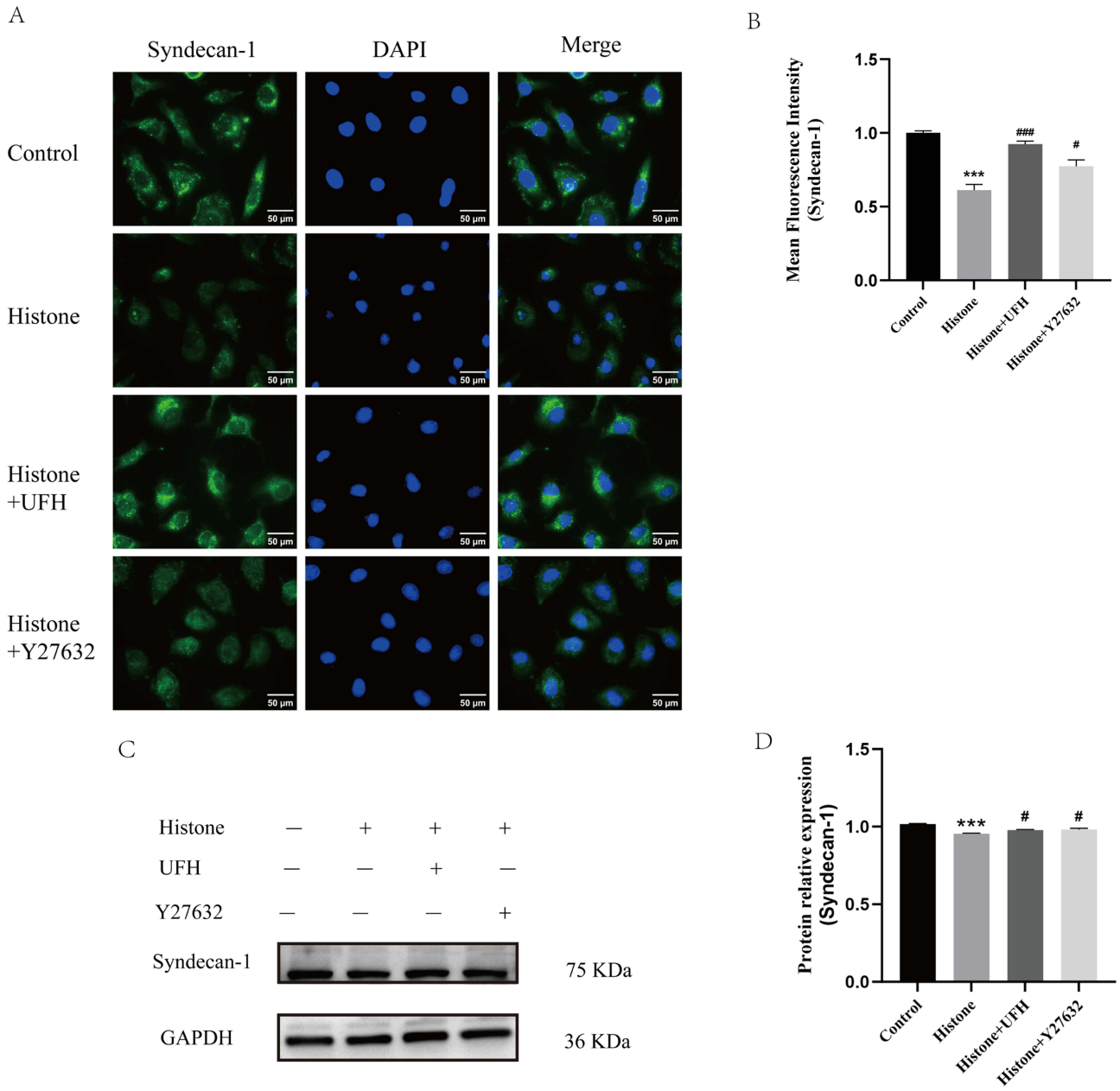

Figure 2 Effect of UFH or Y27632 pretreatment on histone-induced syndecan-1 shedding in HPMECs. (**A**) Syndecan-1 was examined by immunofluorescence staining with Alexa Fluor® 488. (**B**) The mean fluorescence intensity of syndecan-1 in each group (400×). Scale bar = 50 μm. Mean ± SD. n = 3. (**C**) Western blot analysis was used to evaluate the levels of syndecan-1. (**D**) The relative protein expression of syndecan-1 in each group. Mean ± SD. n = 3. $^{***}P < 0.001$, compared with control group; $^{\#}P < 0.05$, compared with histone group; $^{\#\#\#}P < 0.001$, compared with histone group.

levels by quantitative Western blotting. As shown in Figure 2C and D, Y27632 or UFH pretreatment inhibited the histone-induced decrease in syndecan-1 levels.

Microtubules, composed of α-tubulin and β-tubulin, play an essential role in maintaining cell structure and regulating endothelial barrier function. Immunofluorescence staining of β-tubulin (Figure 3A and B) showed that microtubules were stained green and uniformly distributed in normal cells. Compared with the control group, the expression of β-tubulin in HPMECs was significantly reduced after stimulation with histone, especially that close to the cell membrane. These findings suggest that histone induced microtubule disassembly, whereas pretreatment with UFH or Y27632 attenuated the depolymerization of microtubules in HPMECs.

https://doi.org/10.2147/JIR.S573499

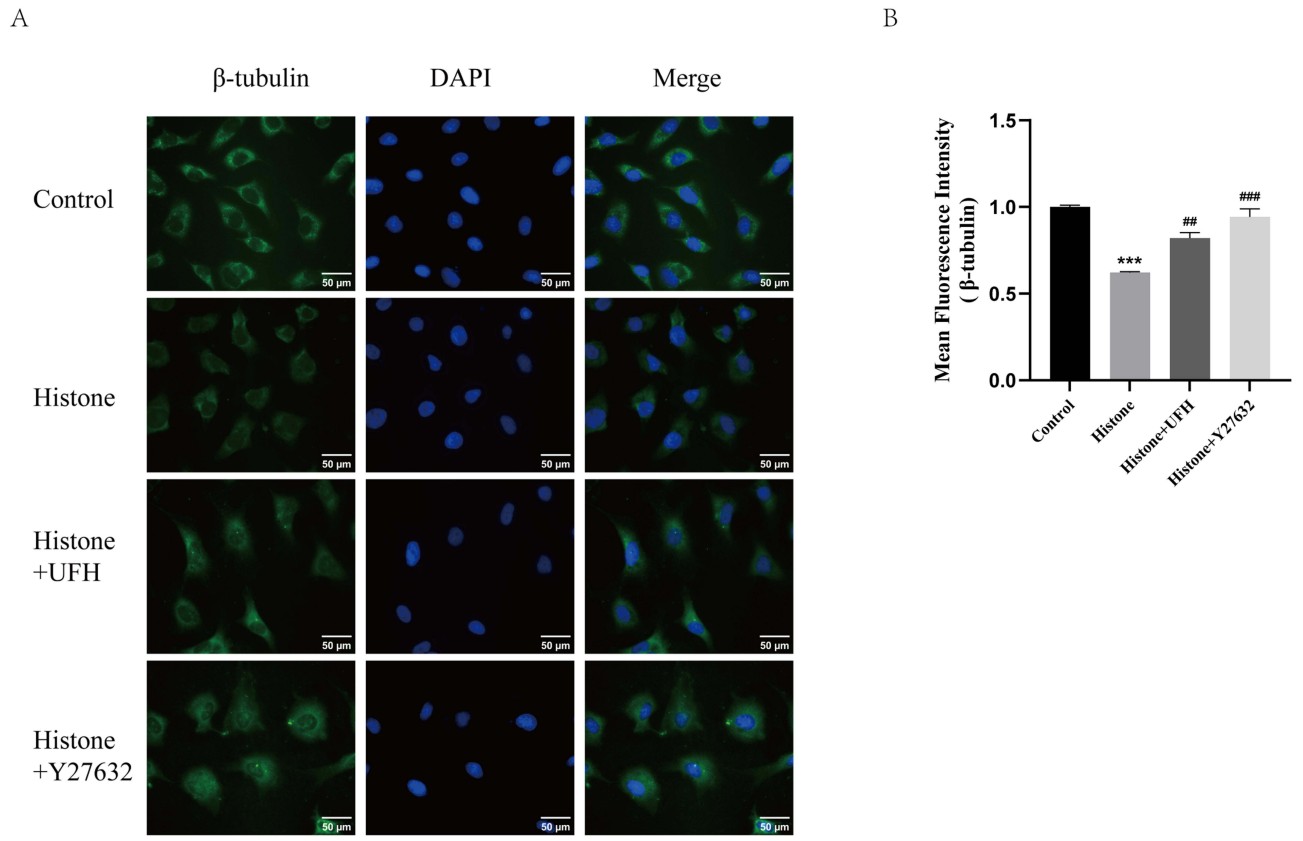

Figure 3 Effect of UFH or Y27632 pretreatment on histone-induced microtubule disassembly in HPMECs. (**A**) β-tubulin was examined by immunofluorescence staining with Alexa Fluor® 488. (**B**) The mean fluorescence intensity of β-tubulin in each group (400×). Scale bar = 50 μm. Mean ± SD. n = 3. ***$P < 0.001$, compared with control group; ##$P < 0.01$, compared with histone group; ####$P < 0.001$, compared with histone group.

Acetylated tubulin is the stable form of microtubules. Similar changes were observed in immunofluorescence staining of acetylated tubulin. As shown in Figure 4A and B, the acetylated microtubule structures in the control group were stained green and uniformly distributed in cells. Compared with normal cells, histone stimulation caused a decrease in the level of tubulin acetylation, especially in regions close to the cell membrane periphery. UFH and Y27632 pretreatment inhibited the histone-induced reduction in acetylated tubulin expression. Furthermore, acetylated tubulin levels were detected by quantitative Western blotting. As shown in Figure 4C and D, Y27632 or UFH pretreatment inhibited the histone-induced decrease in acetylated tubulin levels.

These findings suggest that UFH protects against histone-induced hyperpermeability of HPMECs by attenuating glycocalyx shedding and microtubule disassembly.

Effects of UFH on Histone-Induced HPA-1 Expression, Distribution and Secretion

HPA can destroy the structure of the glycocalyx by cleaving HS chains. Immunofluorescence was used to detect the translocation of HPA-1. As shown in Figure 5A and B, in the resting state, HPA-1 was distributed close to the nucleus. Histone stimulation resulted in enhanced expression of HPA-1 and its translocation from the perinuclear region to the membrane of HPMECs. The levels of HPA-1 expression and translocation were decreased in UFH- and Y27632-pretreated cells.

Furthermore, ELISA was applied to measure HPA-1 levels in the culture supernatants of HPMECs (Figure 5C). Compared with the control group, histone stimulation increased the level of HPA-1 in the supernatant (19.42±2.03 ng/mL vs 46.97±1.28 ng/mL, $P < 0.05$). Combined with the immunofluorescence results, these findings suggest that histone stimulation leads to increased production and membrane-oriented translocation of HPA-1, which in turn result in subsequent enhanced secretion. Y27632 pretreatment reduced the above changes in HPA-1 secretion from endothelial cells

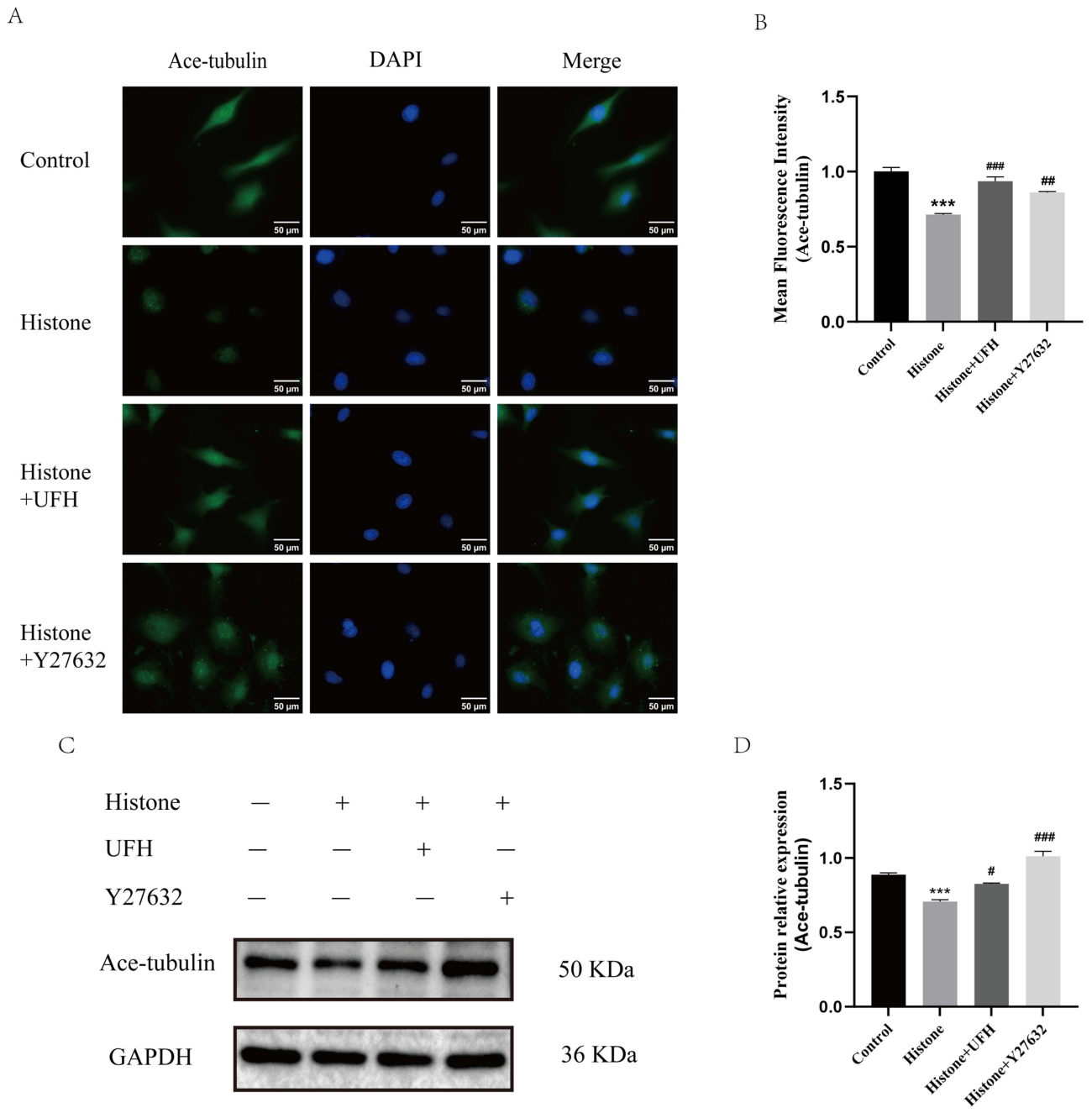

Figure 4 Effect of UFH or Y27632 pretreatment on histone-induced microtubule instability in HPMECs. (**A**) Ace-tubulin was examined by immunofluorescence staining with Alexa Fluor® 488. (**B**) The mean fluorescence intensity of ace-tubulin in each group (400×). Scale bar = 50 μm. Mean ± SD. n = 3. (**C**) Western blot analysis was used to evaluate the levels of Ace-tubulin. (**D**) The relative protein expression of Ace-tubulin in each group. Mean ± SD. n = 3. ***$P < 0.001$, compared with control group; $^{\#}P < 0.05$, compared with histone group; $^{\#\#}P < 0.01$, compared with histone group; $^{\#\#\#}P < 0.001$, compared with histone group.

(36.37±1.53 ng/mL vs 46.97±1.28 ng/mL, $P < 0.05$). UFH pretreatment also decreased the histone-induced increase in HPA-1 levels in HPMECs (35.03±3.39 ng/mL vs 46.97±1.28 ng/mL, $P < 0.05$).

Western blotting was also performed to detect HPA-1 protein expression in HPMECs of each group (Figure 5D and E). Compared with vehicle-treated cells, HPA-1 expression increased after one hour of exposure to histone, whereas UFH and Y27632 inhibited histone-induced HPA-1 expression. This was consistent with the immunofluorescence results.

https://doi.org/10.2147/JIR.S573499

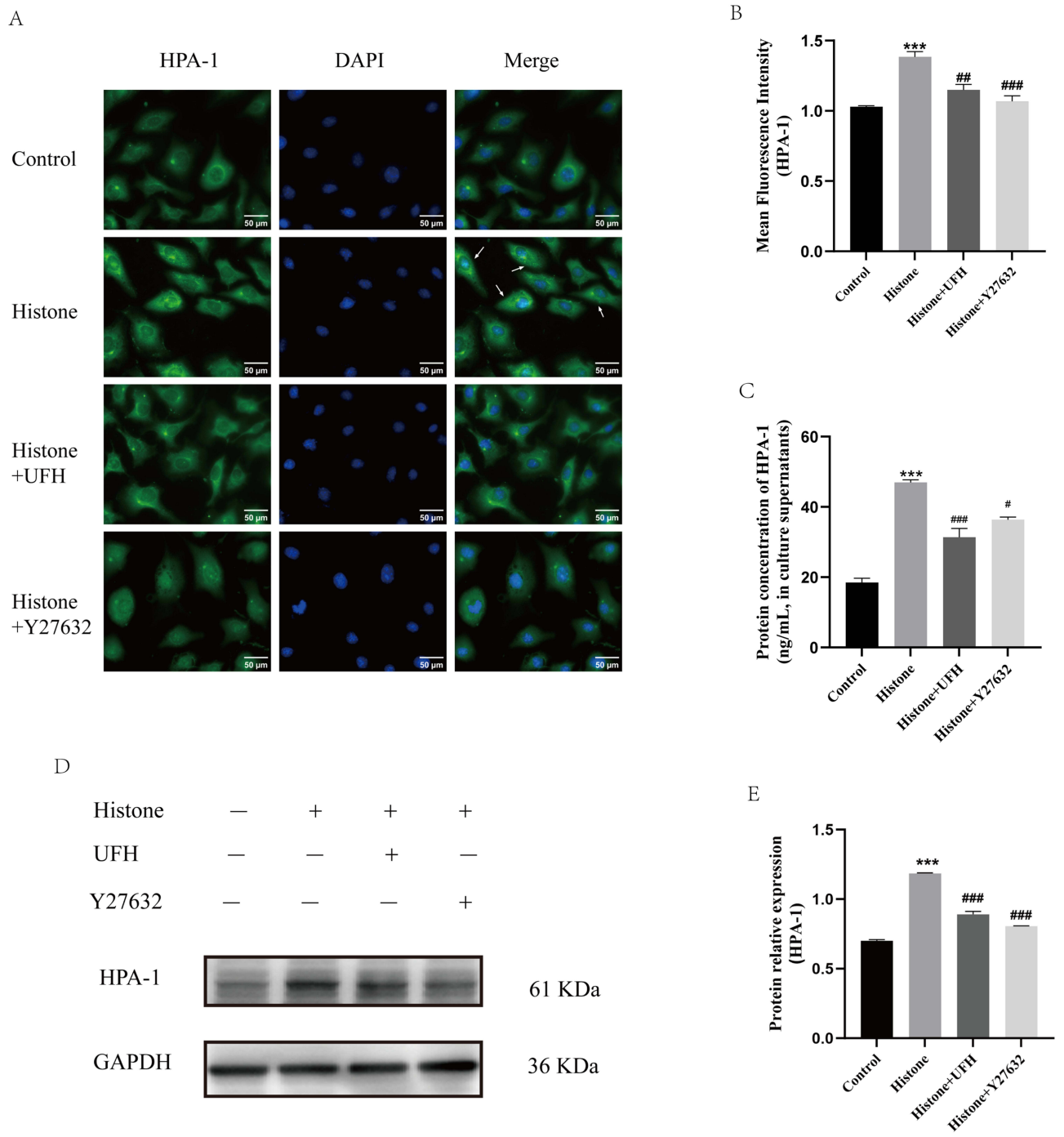

Figure 5 Effects of UFH or Y27632 pretreatment on histone-induced increased expression, translocation and secretion of HPA-1 in HPMECs. (**A**) HPA-1 was examined by immunofluorescence staining with Alexa Fluor® 488. (**B**) The mean fluorescence intensity of HPA-1 in each group (400×). Scale bar = 50 μm. (**C**) The protein levels of HPA-1 in the culture supernatants of HPMECs were examined by ELISA. (**D**) Western blot analysis was used to evaluate the protein levels of HPA-1 in HPMECs. (**E**) The relative protein expression of HPA-1 in HPMECs in each group. Mean ± SD. n = 3. $^{***}P < 0.001$, compared with control group; $^{\#}P < 0.05$, compared with histone group; $^{\#\#}P < 0.01$, compared with histone group; $^{\#\#\#}P < 0.001$, compared with histone group.

UFH Alleviates Histone-Induced Endothelial Barrier Dysfunction and Suppresses HPA-1 Through ROCK Signaling

To further investigate the role of histone in ROCK activation and regulation of cellular dynamics, Western blot was applied to detect the expression of ROCK-1 and p-MLC in HPMECs. The results suggested that ROCK-1 and p-MLC

 https://doi.org/10.2147/JIR.S573499

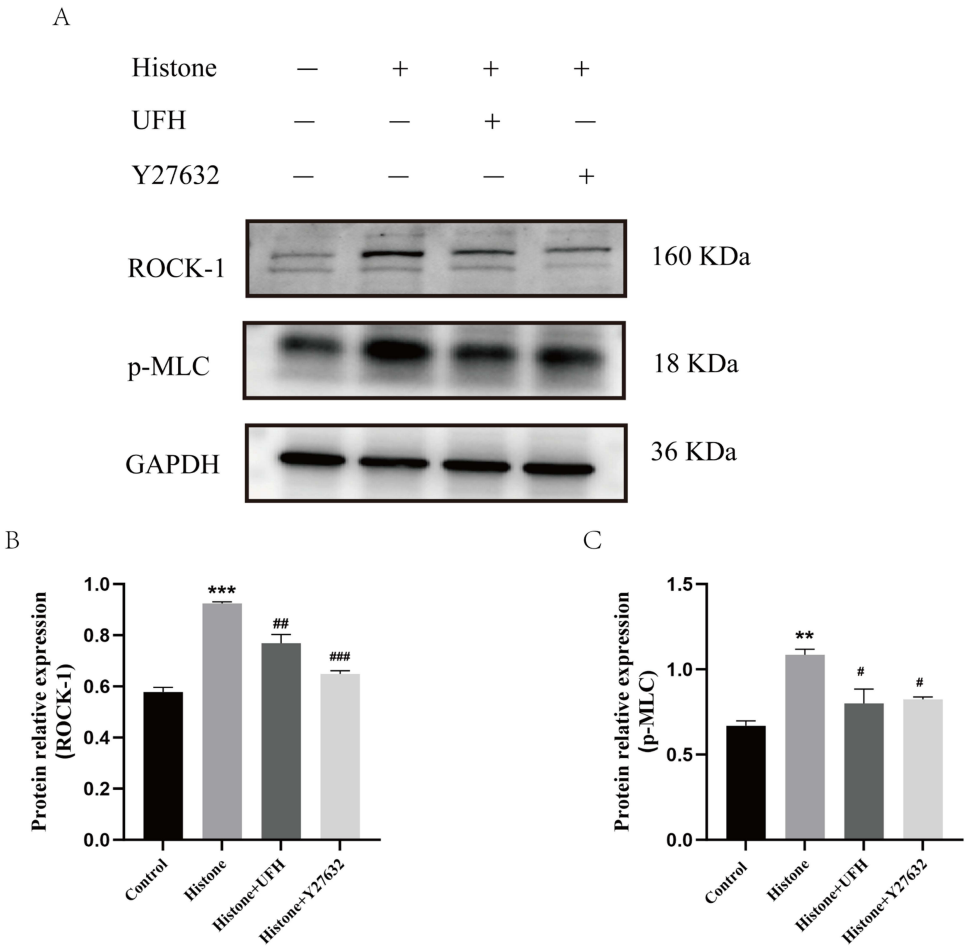

Figure 6 Effects of UFH or Y27632 pretreatment on histone-induced increased expression of ROCK-1 and p-MLC in HPMECs. (**A**) Western blot analysis was used to evaluate the levels of ROCK-1 and p-MLC. (**B**) The relative protein expression of ROCK-1 in each group. (**C**) The relative protein expression of p-MLC in each group. Mean ± SD. n = 3. $^{**}P < 0.01$, compared with control group; $^{***}P < 0.001$, compared with control group; $^{\#}P < 0.05$, compared with histone group; $^{\#\#}P < 0.01$, compared with histone group; $^{\#\#\#}P < 0.001$, compared with histone group.

expression were enhanced after histone stimulation (Figure 6A–C). ROCK inhibitor pretreatment reduced histone-induced MLC phosphorylation. UFH pretreatment decreased histone-induced ROCK-1 expression and MLC phosphorylation in HPMECs. These results suggested that UFH alleviated the effects of histone on the cellular dynamics of HPMECs through the ROCK pathway.

Taken together, these results indicate that UFH attenuates histone-induced glycocalyx shedding and endothelial barrier dysfunction, accompanied by the suppression of histone-induced HPA-1 expression, perinuclear-to-membrane translocation, and secretion, with the involvement of the ROCK pathway.

Discussion

In this study, we showed that histones might induce glycocalyx shedding and endothelial barrier dysfunction via the ROCK pathway, with associated HPA upregulation. Furthermore, UFH might protect the glycocalyx by inhibiting ROCK signaling and HPA expression. To our knowledge, this is the first study to suggest that the ROCK pathway mediates histone-induced glycocalyx degradation, which is associated with HPA upregulation.

Sepsis is a life-threatening clinical syndrome characterized by activation of systemic inflammatory cascade, and potential progression to MODS or death.[35] Previous studies have shown that elevated circulating glycocalyx degradation products correlate with inflammatory mediators, organ damage, and disease severity in septic shock, suggesting the glycocalyx as a molecular target in sepsis.[36] Recent findings in bacterial and viral sepsis further link glycocalyx integrity

https://doi.org/10.2147/JIR.S573499

to systemic inflammatory response severity, underscoring its diagnostic and therapeutic importance.[37] Protecting the endothelial barrier is therefore crucial in sepsis.

Histones are important mediators in sepsis pathogenesis.[38] They activate multiple signaling pathways, promote inflammation and coagulation/fibrinolysis imbalance, and cause endothelial damage,[39] including toxicity to intestinal microvascular endothelium[40] and disruption of the endothelial glycocalyx, which can lead to pulmonary edema.[8] In the present in vitro study, we confirmed that histones caused destabilization and disruption of microtubules, disrupted the glycocalyx, and impaired endothelial barrier function, consistent with our previous in vivo findings.[8]

HPA degrades heparan sulfate side chains of the glycocalyx[41] and is highly expressed in sepsis, tumors, and diabetes.[42,43] Our previous work demonstrated that histones upregulate HPA mRNA and protein, leading to glycocalyx disruption in mouse pulmonary endothelium.[8] However, how histones regulate HPA function remains unclear. Here we found that histones increased HPA protein expression in HPMECs, and immunofluorescence revealed that histones induce HPA translocation from the nucleus to the cell membrane. Moreover, ELISA showed elevated HPA levels in the culture supernatant of histone-treated HPMECs, indicating that histones promote HPA expression, translocation, and release, thereby damaging the glycocalyx. Wang et al reported that high glucose alters cell dynamics and promotes stress fiber reorganization, facilitating HPA translocation from the nucleus to the cell membrane.[24] Whether cell dynamics regulate HPA in sepsis, particularly under histone stimulation, has not been reported. Therefore, we used a ROCK inhibitor to explore this pathway.

The RhoA/ROCK pathway promotes MLC phosphorylation, myosin remodeling, and stress fiber generation, altering cell dynamics.[44] Microtubules, composed of α- and β-tubulin, depolymerize under pathological conditions, leading to cytoskeleton disruption.[45] Microtubule depolymerization releases GEF-H1, which activates Rho/ROCK and cross-talks with actin, causing cell contraction and increased permeability.[46] Various stimuli such as LPS and HMGB1 activate Rho/ROCK and downstream p-MLC, inducing myosin stress fiber formation, microtubule disruption, and increased endothelial permeability.[25,33] These studies indicate that RhoA/ROCK is involved in regulating endothelial barrier function. In this study, histones induced cytoskeleton destruction via the ROCK pathway and increased HPMEC permeability. Of note, syndecan-1 participates in acute mechanosensing in endothelial cells in response to shear stress, as its deficiency impairs Protein Kinase B (Akt) and RhoA activation.[47] Moreover, syndecan-1 has been reported to ameliorate acute lung injury via the RhoA/ROCK pathway.[48] These findings support the notion that ROCK serves as a key signaling hub linking histones to syndecan-1 regulation.

Actin remodeling into stress fibers can serve as tracks for vesicular transport from the nucleus to the plasma membrane,[49] and microtubule instability synergistically promotes this polar transport and secretion.[50] We found that histones disrupted the glycocalyx through the ROCK pathway, but how this process regulates HPA was unclear. Wang et al[24] linked high glucose-induced cell dynamics changes (stress fiber formation) to HPA secretion, suggesting that cell dynamics regulate HPA. Our results showed that histones caused microtubule cytoskeleton destruction, which was associated with increased HPA expression, displacement, and release. ROCK inhibition attenuated these changes, reduced glycocalyx damage, improved endothelial permeability, and protected the barrier. Taken together, these findings provide preliminary evidence suggesting that histones may induce HPA-mediated glycocalyx damage via the ROCK pathway in HPMECs.

UFH is widely used clinically as an anticoagulant.[51] Its non-anticoagulant effects in sepsis, including inhibition of inflammatory responses, have attracted increasing attention.[30] We previously found that UFH ameliorates histone-induced glycocalyx shedding and pulmonary edema in mice.[8] Others reported that UFH reduces LPS-induced ROCK-1 expression and protects the lung endothelial barrier.[52] Consistently, our present study shows that UFH attenuates histone-mediated glycocalyx and microtubule damage and reduces endothelial leakage in HPMECs, thereby protecting the endothelial barrier. This protective effect is closely related to the regulation of HPA. Indeed, our previous work demonstrated that UFH not only inhibits inflammation and stabilizes coagulation but also protects the glycocalyx by inhibiting the histone-mediated HPA pathway.[8] Structurally similar to HS, UFH can compete with HPA for binding on the cell membrane, thus protecting the HS chain and the glycocalyx.[53] In addition to this direct competition, we also found that UFH down-regulates histone-mediated HPA mRNA and protein expression in mice, suggesting that UFH also regulates HPA through intracellular signaling pathways.[8]

This study has several limitations. First, UFH pretreatment (aiming to mitigate histone toxicity) does not fully replicate the clinical scenario. Second, as an in vitro cell model, it cannot recapitulate the complex multi-factor interactions in animals or humans. Third, only a single time point was examined; dynamic changes of the indicators were not assessed. Fourth, we used unfractionated total histone preparations (Sigma H9250), a mixture, rather than purified individual isotypes. Future studies using recombinant individual histones are needed to identify which isotype(s) mediate the observed effects. Nevertheless, since sepsis involves simultaneous release of multiple histone subtypes, the mixed preparation retains pathophysiological relevance.

Conclusion

In summary, our study indicates that UFH protects the glycocalyx and endothelial barrier while inhibiting histone-induced HPA expression, perinuclear distribution, and secretion, with the involvement of the ROCK pathway. These findings may provide a new therapeutic strategy for sepsis.

Data Sharing Statement

No datasets were generated or analysed during the current study.

Ethics Approval and Consent to Participate

This study complies with the Declaration of Helsinki.

Author Contributions

Xinghua Li: conceptualization, methodology, writing – original draft, writing – review and editing.

Yawen Chi: methodology, writing – review and editing.

Mengke Zhuo: formal analysis, investigation, writing – review and editing.

Xin Li: formal analysis, investigation, writing – review and editing.

Chengrui Zhu: data curation, funding acquisition, writing – review and editing.

Xu Li: conceptualization, funding acquisition, writing – review and editing.

All authors gave final approval of the version to be published; have agreed on the journal to which the article has been submitted; and agree to be accountable for all aspects of the work.

Funding

This work was supported by the National Natural Science Foundation of China (82272195); the Department of Science and Technology of Liaoning Province (2023-MS-193).

Disclosure

The authors declare no competing interests.

References

1. Singer M, Deutschman CS, Seymour CW, et al. The third international consensus definitions for sepsis and septic shock (Sepsis-3). *JAMA*. 2016;315(8):801–810. doi:10.1001/jama.2016.0287
2. Rudd KE, Johnson SC, Agesa KM, et al. Global, regional, and national sepsis incidence and mortality, 1990-2017: analysis for the global burden of disease study. *Lancet*. 2020;395(10219):200–211. doi:10.1016/S0140-6736(19)32989-7
3. Venkatesh S, Workman JL. Histone exchange, chromatin structure and the regulation of transcription. *Nat Rev Mol Cell Biol*. 2015;16(3):178–189. doi:10.1038/nrm3941
4. Silk E, Zhao H, Weng H, et al. The role of extracellular histone in organ injury. *Cell Death Dis*. 2017;8(5):e2812. doi:10.1038/cddis.2017.52
5. Nicolaes GAF, Soehnlein O. Targeting extranuclear histones to alleviate acute and chronic inflammation. *Trends Pharmacol Sci*. 2024;45(7):651–662. doi:10.1016/j.tips.2024.05.008
6. Li L, Yu S, Fu S, et al. Unfractionated heparin inhibits histone-mediated coagulation activation and thrombosis in mice. *Thromb Res*. 2020;193:122–129. doi:10.1016/j.thromres.2020.06.007
7. Xu J, Zhang X, Pelayo R, et al. Extracellular histones are major mediators of death in sepsis. *Nat Med*. 2009;15(11):1318–1321. doi:10.1038/nm.2053

8. Fu S, Yu S, Zhao Y, et al. Unfractionated heparin attenuated histone-induced pulmonary syndecan-1 degradation in mice: a preliminary study on the roles of heparinase pathway. *Inflammation*. 2022;45(2):712–724. doi:10.1007/s10753-021-01578-w
9. Wang W. Change in properties of the glycocalyx affects the shear rate and stress distribution on endothelial cells. *J Biomech Eng*. 2007;129 (3):324–329. doi:10.1115/1.2720909
10. Becker BF, Jacob M, Leipert S, et al. Degradation of the endothelial glycocalyx in clinical settings: searching for the sheddases. *Br J Clin Pharmacol*. 2015;80(3):389–402. doi:10.1111/bcp.12629
11. Kunnathattil M, Rahul P, Skaria T. Soluble vascular endothelial glycocalyx proteoglycans as potential therapeutic targets in inflammatory diseases. *Immunol Cell Biol*. 2024;102(2):97–116. doi:10.1111/imcb.12712
12. Tanino Y, Chang MY, Wang X, et al. Syndecan-4 regulates early neutrophil migration and pulmonary inflammation in response to lipopolysaccharide. *Am J Respir Cell Mol Biol*. 2012;47(2):196–202. doi:10.1165/rcmb.2011-0294OC
13. Vuong TT, Reine TM, Sudworth A, et al. Syndecan-4 is a major syndecan in primary human endothelial cells in vitro, modulated by inflammatory stimuli and involved in wound healing. *J Histochem Cytochem*. 2015;63(4):280–292. doi:10.1369/0022155415568995
14. Suzuki K, Okada H, Takemura G, et al. Recombinant thrombomodulin protects against LPS-induced acute respiratory distress syndrome via preservation of pulmonary endothelial glycocalyx. *Br J Pharmacol*. 2020;177(17):4021–4033. doi:10.1111/bph.15153
15. Yin J, Chi Y, Liu D, et al. Unfractionated heparin attenuated histone-induced pulmonary endothelial glycocalyx injury through Ang/Tie2 pathway. *J Inflamm*. 2025;22(1):9. doi:10.1186/s12950-025-00437-x
16. Sebestyén A, Gallai M, Knittel T, et al. Cytokine regulation of syndecan expression in cells of liver origin. *Cytokine*. 2000;12(10):1557–1560. doi:10.1006/cyto.2000.0754
17. Xu J, Park PW, Kheradmand F, et al. Endogenous attenuation of allergic lung inflammation by syndecan-1. *J Immunol*. 2005;174(9):5758–5765. doi:10.4049/jimmunol.174.9.5758
18. Hayashida K, Parks WC, Park PW. Syndecan-1 shedding facilitates the resolution of neutrophilic inflammation by removing sequestered CXC chemokines. *Blood*. 2009;114(14):3033–3043. doi:10.1182/blood-2009-02-204966
19. Goodall KJ, Poon IK, Phipps S, et al. Soluble heparan sulfate fragments generated by heparanase trigger the release of pro-inflammatory cytokines through TLR-4. *PLoS One*. 2014;9(10):e109596. doi:10.1371/journal.pone.0109596
20. Keyloun JW, Le TD, Pusateri AE, et al. Circulating syndecan-1 and tissue factor pathway inhibitor, biomarkers of endothelial dysfunction, predict mortality in burn patients. *Shock*. 2021;56(2):237–244. doi:10.1097/SHK.0000000000001709
21. Rovas A, Seidel LM, Vink H, et al. Association of sublingual microcirculation parameters and endothelial glycocalyx dimensions in resuscitated sepsis. *Crit Care*. 2019;23(1):260. doi:10.1186/s13054-019-2542-2
22. Peterson SB, Liu J. Unraveling the specificity of heparanase utilizing synthetic substrates. *J Biol Chem*. 2010;285(19):14504–14513. doi:10.1074/jbc.M110.104166
23. Wang D, Wang K, Liu Q, et al. A novel drug candidate for sepsis targeting heparanase by inhibiting cytokine storm. *Adv Sci*. 2024;11(29): e2403337. doi:10.1002/advs.202403337
24. Wang F, Wang Y, Kim MS, et al. Glucose-induced endothelial heparanase secretion requires cortical and stress actin reorganization. *Cardiovasc Res*. 2010;87(1):127–136. doi:10.1093/cvr/cvq051
25. Mu S, Liu Y, Jiang J, et al. Unfractionated heparin ameliorates pulmonary microvascular endothelial barrier dysfunction via microtubule stabilization in acute lung injury. *Respir Res*. 2018;19(1):220. doi:10.1186/s12931-018-0925-6
26. Ebeyer-Masotta M, Eichhorn T, Weiss R, et al. Heparin-functionalized adsorbents eliminate central effectors of immunothrombosis, including platelet factor 4, high-mobility group box 1 protein and histones. *Int J Mol Sci*. 2022;23(3):1823. doi:10.3390/ijms23031823
27. Alsagaff MY, Mulia EPB, Maghfirah I, et al. Low molecular weight heparin is associated with better outcomes than unfractionated heparin for thromboprophylaxis in hospitalized COVID-19 patients: a meta-analysis. *Eur Heart J Qual Care Clin Outcomes*. 2022;8(8):909–918. doi:10.1093/ehjqcco/qcac046
28. Li X, Ma X. The role of heparin in sepsis: much more than just an anticoagulant. *Br J Haematol*. 2017;179(3):389–398. doi:10.1111/bjh.14885
29. Yu S, Chi Y, Ma X, et al. Heparin in sepsis: current clinical findings and possible mechanisms. *Front Immunol*. 2024;15:1495260. doi:10.3389/fimmu.2024.1495260
30. Tang Y, Wang X, Li Z, et al. Heparin prevents caspase-11-dependent septic lethality independent of anticoagulant properties. *Immunity*. 2021;54 (3):454–467.e6. doi:10.1016/j.immuni.2021.01.007
31. Li X, Zheng Z, Mao Y, et al. Unfractionated heparin promotes LPS-induced endothelial barrier dysfunction: a preliminary study on the roles of angiopoietin/Tie2 axis. *Thromb Res*. 2012;129(5):e223–e228. doi:10.1016/j.thromres.2012.03.003
32. Zhu C, Liang Y, Li X, et al. Unfractionated heparin attenuates histone-mediated cytotoxicity in vitro and prevents intestinal microcirculatory dysfunction in histone-infused rats. *J Trauma Acute Care Surg*. 2019;87(3):614–622. doi:10.1097/TA.0000000000002387
33. Zhao MJ, Jiang HR, Sun JW, et al. Roles of RAGE/ROCK1 pathway in HMGB1-induced early changes in barrier permeability of human pulmonary microvascular endothelial cell. *Front Immunol*. 2021;12:697071. doi:10.3389/fimmu.2021.697071
34. Liu Z, Chen M, Sun Y, et al. Transforming growth factor-β receptor type 2 is required for heparin-binding protein-induced acute lung injury and vascular leakage for transforming growth factor-β/Smad/Rho signaling pathway activation. *FASEB J*. 2022;36(11):e22580. doi:10.1096/fj.202200228RRRRR
35. Rovas A, Sackarnd J, Rossaint J, et al. Identification of novel sublingual parameters to analyze and diagnose microvascular dysfunction in sepsis: the NOSTRADAMUS study. *Crit Care*. 2021;25(1):112. doi:10.1186/s13054-021-03520-w
36. Yini S, Heng Z, Xin A, et al. Effect of unfractionated heparin on endothelial glycocalyx in a septic shock model. *Acta Anaesthesiol Scand*. 2015;59 (2):160–169. doi:10.1111/aas.12418
37. Rovas A, Buscher K, Osiaevi I, et al. Microvascular and proteomic signatures overlap in COVID-19 and bacterial sepsis: the MICROCODE study. *Angiogenesis*. 2022;25(4):503–515. doi:10.1007/s10456-022-09843-8
38. Ligi D, Lo Sasso B, Giglio RV, et al. Circulating histones contribute to monocyte and MDW alterations as common mediators in classical and COVID-19 sepsis. *Crit Care*. 2022;26(1):260. doi:10.1186/s13054-022-04138-2
39. Luo G, Liu B, Fu T, et al. The role of histone deacetylases in acute lung injury-friend or foe. *Int J Mol Sci*. 2023;24(9):7876. doi:10.3390/ijms24097876

40. Zhu C, Liang Y, Liu Y, et al. Unfractionated heparin protects microcirculation in endotoxemic rats by antagonizing histones. *J Surg Res*. 2023;282:84–92. doi:10.1016/j.jss.2022.09.019
41. Bauer C, Piani F, Banks M, et al. Minimal change disease is associated with endothelial glycocalyx degradation and endothelial activation. *Kidney Int Rep*. 2021;7(4):797–809. doi:10.1016/j.ekir.2021.11.037
42. Chen S, Zhang X, Sun Y, et al. Unfractionated heparin attenuates intestinal injury in mouse model of sepsis by inhibiting heparanase. *Int J Clin Exp Pathol*. 2015;8(5):4903–4912.
43. Masola V, Maran C, Tassone E, et al. Heparanase activity in alveolar and embryonal rhabdomyosarcoma: implications for tumor invasion. *BMC Cancer*. 2009;9(1):304. doi:10.1186/1471-2407-9-304
44. Vandenbroucke E, Mehta D, Minshall R, et al. Regulation of endothelial junctional permeability. *Ann N Y Acad Sci*. 2008;1123:134–145. doi:10.1196/annals.1420.016
45. Karki P, Ke Y, Tian Y, et al. Staphylococcus aureus-induced endothelial permeability and inflammation are mediated by microtubule destabilization. *J Biol Chem*. 2019;294(10):3369–3384. doi:10.1074/jbc.RA118.004030
46. Akhshi TK, Wernike D, Piekny A. Microtubules and actin crosstalk in cell migration and division. *Cytoskeleton*. 2014;71(1):1–23. doi:10.1002/cm.21150
47. Voyvodic PL, Min D, Liu R, et al. Loss of syndecan-1 induces a pro-inflammatory phenotype in endothelial cells with a dysregulated response to atheroprotective flow. *J Biol Chem*. 2014;289(14):9547–9559. doi:10.1074/jbc.M113.541573
48. Zhang C, Guo F, Chang M, et al. Exosome-delivered syndecan-1 rescues acute lung injury via a FAK/p190RhoGAP/RhoA/ROCK/NF-κB signaling axis and glycocalyx enhancement. *Exp Cell Res*. 2019;384(1):111596. doi:10.1016/j.yexcr.2019.111596
49. Miklavc P, Frick M. Actin and myosin in non-neuronal exocytosis. *Cells*. 2020;9(6):1455. doi:10.3390/cells9061455
50. Müller MT, Schempp R, Lutz A, et al. Interaction of microtubules and actin during the post-fusion phase of exocytosis. *Sci Rep*. 2019;9(1):11973. doi:10.1038/s41598-019-47741-0
51. Man C, An Y, Wang GX, et al. Recent advances in pathogenesis and anticoagulation treatment of sepsis-induced coagulopathy. *J Inflamm Res*. 2025;18:737–750. doi:10.2147/JIR.S495223
52. Han J, Ding R, Zhao D, et al. Unfractionated heparin attenuates lung vascular leak in a mouse model of sepsis: role of RhoA/Rho kinase pathway. *Thromb Res*. 2013;132(1):e42–e47. doi:10.1016/j.thromres.2013.03.010
53. Schmidt EP, Yang Y, Janssen WJ, et al. The pulmonary endothelial glycocalyx regulates neutrophil adhesion and lung injury during experimental sepsis. *Nat Med*. 2012;18(8):1217–1223. doi:10.1038/nm.2843